

ALGORITHMS FOR APPROXIMATION WITH LOCALLY SUPPORTED RATIONAL SPLINE PREWAVELETS ON THE SPHERE

DANIELA ROȘCA

Abstract. In [5], some locally supported rational spline prewavelets on the sphere were constructed. We present here another two properties of them and some algorithms for decomposition, reconstruction and approximation, together with some numerical tests. A comparison with the spherical harmonics approach shows the advantage of the small support of our prewavelets.

1. Introduction

Consider the unit sphere \mathbb{S}^2 of \mathbb{R}^3 , $\mathbb{S}^2 = \{\mathbf{x} \in \mathbb{R}^3 : \|\mathbf{x}\| = 1\}$. In [5] the following construction were made.

We considered the polyhedron Π having the bound Ω , the vertices situated on \mathbb{S}^2 and triangular faces such that no face contains the origin O and O is situated inside the polyhedron. The set of its faces was denoted $\mathcal{T}^0 = \{T_1^0, T_2^0, \dots, T_n^0\}$. Then we projected each triangle of \mathcal{T}^0 onto \mathbb{S}^2 , getting a triangulation of the sphere, denoted $\mathcal{U}^0 = \{U_1^0, U_2^0, \dots, U_n^0\}$, where $U_i^0 = p(T_i^0)$ and $p: \Omega \rightarrow \mathbb{S}^2$, is the radial projection

$$p(x, y, z) = \left(\frac{x}{\sqrt{x^2 + y^2 + z^2}}, \frac{y}{\sqrt{x^2 + y^2 + z^2}}, \frac{z}{\sqrt{x^2 + y^2 + z^2}} \right), \text{ for all } (x, y, z) \in \Omega.$$

We divided each triangle T_k^0 into four triangles, taking the mid-points of the edges. Thus, we obtained a refined triangulation of Ω , denoted $\mathcal{T}^1 = \{T_1^1, T_2^1, \dots, T_{4n}^1\}$. Continuing the refinement process we built the triangulations \mathcal{T}^j for arbitrary level $j \in \mathbb{N}$. The projection $\mathcal{U}^j = p(\mathcal{T}^j)$ is a triangulation of \mathbb{S}^2 . We denoted by V^j the set of all vertices of plane triangles in \mathcal{T}^j .

Let $M_1 M_i M_k$ be a triangle of \mathcal{T}^j , with the vertices of coordinates (x_1, y_1, z_1) , (x_i, y_i, z_i) , (x_k, y_k, z_k) respectively. Let $M_1' M_i' M_k'$ be its radial projection onto \mathbb{S}^2 . Then we defined the functions $\varphi_{M_1}^j$, associated to the vertex M_1 , as

$$\varphi_{M_1}^j(\eta_1, \eta_2, \eta_3) = \begin{cases} \begin{vmatrix} \eta_1 & \eta_2 & \eta_3 & 0 \\ x_1 & y_1 & z_1 & 1 \\ x_i & y_i & z_i & 1 \\ x_k & y_k & z_k & 1 \end{vmatrix}^{-1}, & \text{on each triangle } M_1' M_i' M_k' \text{ of } \mathcal{U}^j, \\ 0, & \text{on the triangles of } \mathcal{U}^j \text{ that do not contain } M_1'. \end{cases}$$

It is immediately that the function $\varphi_{M_1}^j$ is continuous on \mathbb{S}^2 and the set $\{\varphi_v^j, v \in V^j\}$ is a basis of the space $\mathcal{V}^j = \text{span}\{\varphi_v^j, v \in V^j\}$. We denoted by V_v^j the set of the j -level neighbors of the vertex v .

Due to the refinement relation

$$\varphi_v^j = \varphi_v^{j+1} + \frac{1}{2} \sum_{w \in V_v^{j+1}} \varphi_w^{j+1}, \quad v \in V^j, \quad j \in \mathbb{N},$$

we deduce that $\mathcal{V}^j \subseteq \mathcal{V}^{j+1}$. Then we defined an inner product on \mathbb{S}^2 based on the coarsest triangulation \mathcal{T}^0 :

$$\begin{aligned} \langle F, G \rangle_* &= \langle F \circ p, G \circ p \rangle_\Omega \\ &= \sum_{T \in \mathcal{T}^0} \int_{p(T)} F(\boldsymbol{\eta}) G(\boldsymbol{\eta}) \frac{2d_T^2}{|a_T \eta_1 + b_T \eta_2 + c_T \eta_3|^3} d\omega(\boldsymbol{\eta}), \end{aligned}$$

where $\boldsymbol{\eta} = (\eta_1, \eta_2, \eta_3)$, the numbers a_T, b_T, c_T, d_T are the coefficients of x, y, z and 1 of the polynomial function

$$\begin{vmatrix} x & y & z & 1 \\ x_1 & y_1 & z_1 & 1 \\ x_2 & y_2 & z_2 & 1 \\ x_3 & y_3 & z_3 & 1 \end{vmatrix}$$

and the triangle T has the vertices $M_i(x_i, y_i, z_i)$, $i = 1, 2, 3$. The inner product $\langle \cdot, \cdot \rangle_*$ may be interpreted as a “multi-weighted” inner product, with the weights

$$w_T(\eta_1, \eta_2, \eta_3) = \frac{2d_T^2}{|a_T \eta_1 + b_T \eta_2 + c_T \eta_3|^3}. \quad (1)$$

Afterwards and we considered the space \mathcal{W}^j as the orthogonal complement of \mathcal{V}^j into \mathcal{V}^{j+1} :

$$\mathcal{V}^{j+1} = \mathcal{V}^j \oplus \mathcal{W}^j. \quad (2)$$

The spaces \mathcal{W}^j were called the *wavelet spaces*. We determined a basis in each \mathcal{W}^j , consisting of prewavelets of small supports. This basis consists in the following functions:

$$\psi_u^j(\boldsymbol{\eta}) = \sigma_{a_1, u}^j(\boldsymbol{\eta}) + \sigma_{a_2, u}^j(\boldsymbol{\eta}), \quad (3)$$

with

$$\begin{aligned} \sigma_{a_1, u}^j(\boldsymbol{\eta}) &= s_{a_1} \varphi_{a_1}^{j+1}(\boldsymbol{\eta}) + \sum_{w \in V_{a_1}^{j+1}} s_w \varphi_w^{j+1}(\boldsymbol{\eta}), \\ \sigma_{a_2, u}^j(\boldsymbol{\eta}) &= s_{a_2} \varphi_{a_2}^{j+1}(\boldsymbol{\eta}) + \sum_{w \in V_{a_2}^{j+1}} t_w \varphi_w^{j+1}(\boldsymbol{\eta}), \end{aligned}$$

where u is a “new” vertex, mid-point of the edge $[a_1 a_2]$, $s_{a_1} = -\frac{3}{2s_1}$, $s_{a_2} = -\frac{3}{2s_2}$, $s_{b_i} = \frac{3}{28s_1} + \theta(i, s_1)$, $t_{c_i} = \frac{3}{28s_2} + \theta(i, s_2)$. Here s_1 and s_2 are the number of neighbors of the vertices a_1 resp. a_2 , $\theta(i, s) = \frac{\lambda^i + \lambda^{s-i}}{\sqrt{21}(1-\lambda^s)}$, $\lambda = \frac{-5+\sqrt{21}}{2}$. By $b_0, b_1, \dots, b_{s_1-1}$ we denoted the ordered neighbors of a_1 , starting with $b_0 = u$ and by $c_0, c_1, \dots, c_{s_2-1}$ we denoted the ordered neighbors of a_2 , starting with $c_0 = u$.

The set $\{\psi_u^j, u \in V^{j+1} \setminus V^j\}$ was proved to be a stable basis of $L^2(\mathbb{S}^2)$ (see [5], Section 3).

In the next section we present the algorithms of decomposition and reconstruction.

2. Decomposition and reconstruction

Consider $\{\varphi_v^j\}_{v \in V^j}$ basis of \mathcal{V}^j and $\{\psi_u^j\}_{u \in V^{j+1} \setminus V^j}$ basis of \mathcal{W}^j . With a fixed ordering of the vertices in V^j and in $V^{j+1} \setminus V^j$, we can regard these bases as row vectors:

$$\Phi^j = (\varphi_v^j)_{v \in V^j} \quad \text{and} \quad \Psi^j = (\psi_u^j)_{u \in V^{j+1} \setminus V^j}.$$

Then any elements $f^j = \sum_{v \in V^j} f_v^j \varphi_v^j$ and $g^j = \sum_{u \in V^{j+1} \setminus V^j} g_u^j \psi_u^j$ in \mathcal{V}^j resp. \mathcal{W}^j can be written as

$$f^j = \Phi^j \mathbf{f}^j \quad \text{resp.} \quad g^j = \Psi^j \mathbf{g}^j, \quad (4)$$

where \mathbf{f}^j is the column vector $(f_v^j)_{v \in V^j}$ and \mathbf{g}^j is the column vector $(g_u^j)_{u \in V^{j+1} \setminus V^j}$.

Since \mathcal{V}^{j-1} and \mathcal{W}^{j-1} are subspaces of \mathcal{V}^j , there exist two unique matrices P^j and Q^j such that

$$\Phi^{j-1} = \Phi^j P^j \quad \text{and} \quad \Psi^{j-1} = \Phi^j Q^j. \quad (5)$$

Take now $f^j \in \mathcal{V}^j$. Equation (2) implies that there exist unique $f^{j-1} \in \mathcal{V}^{j-1}$ and $g^{j-1} \in \mathcal{W}^{j-1}$ such that

$$f^j = f^{j-1} + g^{j-1}. \quad (6)$$

Substituting (4) into (6) yields the following equation:

$$\Phi^j \mathbf{f}^j = \Phi^{j-1} \mathbf{f}^{j-1} + \Psi^{j-1} \mathbf{g}^{j-1}$$

and then, using (5) and the fact that Φ^j is a basis for \mathcal{V}^j , we find

$$(P^j \ Q^j) \begin{pmatrix} \mathbf{f}^{j-1} \\ \mathbf{g}^{j-1} \end{pmatrix} = \mathbf{f}^j. \quad (7)$$

The block matrix $(P^j \ Q^j)$ is called the *two-scaled matrix*. It is nonsingular and it must be inverted in order to compute the coefficient vectors \mathbf{f}^{j-1} and \mathbf{g}^{j-1} from a given coefficient vector \mathbf{f}^j . Repeating the above calculations for the levels $j = m, m-1, \dots, 1$, we obtain the decomposition algorithm.

Algorithm D

Input : $m \in \mathbb{N}$ highest level
 $\mathbf{f}^m = (f_v^m)_{v \in V^m}$ the values of a given function $f^m \in \mathcal{V}^m$
at the nodes $v \in V^m$.

(i) For each level $j = m, m-1, \dots, 1$, solve the linear system (7)
and get \mathbf{f}^{j-1} and \mathbf{g}^{j-1} .

Output : \mathbf{g}^j ($j = 0, 1, \dots, m-1$) wavelet coefficients,
 \mathbf{f}^0 coefficient of approximation.

Thus, the function $f^m \in \mathcal{V}^m$ was decomposed into

$$f^m = f^0 + g^0 + g^1 + \dots + g^{m-1},$$

meaning an approximation $f^0 \in \mathcal{V}^0$ and a sum of details (wavelets) $g^i \in \mathcal{W}^i$, $i = 0, 1, \dots, m-1$.

Let us come back to the system (7). The entries of P^j and Q^j are evaluations of the bases Φ^j resp. Ψ^j . Their expressions are

$$p_{wv}^j = \varphi_v^{j-1}(w) = \begin{cases} 1 & \text{if } w = v, \\ \frac{1}{2} & \text{if } w \in V_v^j, \\ 0 & \text{otherwise} \end{cases}, \text{ resp. } q_{wu}^j = \psi_u^{j-1}(w).$$

The system (7) can be written

$$\begin{pmatrix} I & Q_1^j \\ P_2^j & Q_2^j \end{pmatrix} \begin{pmatrix} \mathbf{f}^{j-1} \\ \mathbf{g}^{j-1} \end{pmatrix} = \begin{pmatrix} \mathbf{f}_1^j \\ \mathbf{f}_2^j \end{pmatrix} \quad (8)$$

Using the Schur complement matrix $\tilde{Q}_2^j = Q_2^j - P_2^j Q_1^j$, we reduce the system (8) to

$$\begin{pmatrix} I & Q_1^j \\ 0 & \tilde{Q}_2^j \end{pmatrix} \begin{pmatrix} \mathbf{f}^{j-1} \\ \mathbf{g}^{j-1} \end{pmatrix} = \begin{pmatrix} \mathbf{f}_1^j \\ \mathbf{f}_2^j - P_2^j \mathbf{f}_1^j \end{pmatrix}.$$

This means that we have to solve the system

$$\tilde{Q}_2^j \mathbf{g}^{j-1} = \mathbf{f}_2^j - P_2^j \mathbf{f}_1^j$$

for computing \mathbf{g}^{j-1} and then calculate \mathbf{f}^{j-1} from the substitution

$$\mathbf{f}^{j-1} = \mathbf{f}_1^j - Q_1^j \mathbf{g}^{j-1}.$$

Besides the lower dimension, the system (8) has also the advantage that is better conditioned than the system (7).

The next step is to write the reconstruction algorithm.

Algorithm R

- Input :** $m \in \mathbb{N}$ highest level
 $\mathbf{g}^j, j = 0, 1, \dots, m-1$ coefficient vectors of a given function $g^j \in \mathcal{W}^j$
 \mathbf{f}^0 coefficient vector of a given function $f^0 \in \mathcal{V}^0$
 For each level $j = 1, 2, \dots, m$
- (i) (a) compute \mathbf{f}_1^j from $\mathbf{f}_1^j = \mathbf{f}^{j-1} + Q_1^j \mathbf{g}^{j-1}$,
 (b) compute \mathbf{f}_2^j from $\mathbf{f}_2^j = P_2^j \mathbf{f}_1^j + \tilde{Q}_2^j \mathbf{g}^{j-1}$

Output : \mathbf{f}^m

The locality of the supports of our bases has the advantage that the matrices P_2^j and \tilde{Q}_2^j are sparse. In P_2^j , on each column we have two nonzero entries and in \tilde{Q}_2^j , on each column and row we have $n = \max\{1, \{2t(v) - 1, v \in V^0\}\}$ nonzero entries. Here $t(v)$ denotes the number of neighbors of the vertex v .

3. Thresholding

A typically application of wavelets is data compression using thresholding. Numerical examples will be given in Section 5.

A given function $f^m \in \mathcal{V}^m$ is first decomposed into its components $f^0, g^0, g^1, \dots, g^{m-1}$, using the algorithm **D**, with Schur complement. The wavelet components $g^j \in \mathcal{W}^j$ are replaced by the functions $\hat{g}^j \in \mathcal{W}^j$, by modifying their coefficients according to a particular strategy (for more details see [7]). Here we use the strategy called *hard thresholding*, which means that for a threshold $thr > 0$, we set, for $u \in V^{j+1} \setminus V^j$,

$$\hat{g}_u^j = \begin{cases} g_u^j, & \text{if } |g_u^j| \geq thr, \\ 0, & \text{otherwise.} \end{cases}$$

The ratio of number of subsequent nonzero coefficients to the total number

$$\frac{\sum_{j=0}^{m-1} |\{u \in V^{j+1} \setminus V^j : \hat{g}_u^j \neq 0\}|}{\sum_{j=0}^{m-1} |V^{j+1} \setminus V^j|}$$

is called the *compression rate*.

Reconstruction with the algorithm **R**, applied to the modified functions \hat{g}^j , yields an approximant $\hat{f}^m \in \mathcal{V}^m$ of the original function f^m , given by

$$\hat{f}^m = f^0 + \hat{g}^0 + \hat{g}^1 + \dots + \hat{g}^{m-1}.$$

The resulting approximation error is

$$e^m = f^m - \hat{f}^m = \sum_{j=0}^{m-1} (g^j - \hat{g}^j).$$

4. Other properties of our prewavelets

We prove here two properties which were not mentioned in [5].

Proposition 1. *The function $\mathbf{1}_{\mathbb{S}^2} : \mathbb{S}^2 \rightarrow \mathbb{R}$, $\mathbf{1}_{\mathbb{S}^2}(\eta) = 1$ for all $\eta \in \mathbb{S}^2$, belongs to the space \mathcal{V}^0 and therefore to all the spaces \mathcal{V}^j . As a consequence, the prewavelets have a vanishing moment of order zero.*

Proof. First we show that on each triangle $U = A_1A_2A_3$ of U^0 , $A_i(x_i, y_i, z_i)$, $i = 1, 2, 3$ we have

$$\varphi_{A_1}^0 + \varphi_{A_2}^0 + \varphi_{A_3}^0 = 1, \quad (9)$$

which is equivalent to

$$\frac{\begin{vmatrix} \eta_1 & \eta_2 & \eta_3 \\ x_2 & y_2 & z_2 \\ x_3 & y_3 & z_3 \end{vmatrix}}{\begin{vmatrix} \eta_1 & \eta_2 & \eta_3 & 0 \\ x_1 & y_1 & z_1 & 1 \\ x_2 & y_2 & z_2 & 1 \\ x_3 & y_3 & z_3 & 1 \end{vmatrix}} + \frac{\begin{vmatrix} \eta_1 & \eta_2 & \eta_3 \\ x_3 & y_3 & z_3 \\ x_1 & y_1 & z_1 \end{vmatrix}}{\begin{vmatrix} \eta_1 & \eta_2 & \eta_3 & 0 \\ x_2 & y_2 & z_2 & 1 \\ x_3 & y_3 & z_3 & 1 \\ x_1 & y_1 & z_1 & 1 \end{vmatrix}} + \frac{\begin{vmatrix} \eta_1 & \eta_2 & \eta_3 \\ x_1 & y_1 & z_1 \\ x_2 & y_2 & z_2 \end{vmatrix}}{\begin{vmatrix} \eta_1 & \eta_2 & \eta_3 & 0 \\ x_3 & y_3 & z_3 & 1 \\ x_1 & y_1 & z_1 & 1 \\ x_2 & y_2 & z_2 & 1 \end{vmatrix}} = 1$$

for all $(\eta_1, \eta_2, \eta_3) \in U$. This is immediately if we split the determinant from the denominator after the last column.

Now let us take an arbitrary point (η_1, η_2, η_3) of the sphere. It will be situated on a spherical triangle $\tilde{U} \in U^0$ having the vertices M'_1, M'_2, M'_3 , which are the projections of the points M_1, M_2, M_3 , situated on the polyhedron. Then we can write

$$1 = \mathbf{1}_{S^2}(\eta_1, \eta_2, \eta_3) = \varphi_{M'_1}^0(\eta_1, \eta_2, \eta_3) + \varphi_{M'_2}^0(\eta_1, \eta_2, \eta_3) + \varphi_{M'_3}^0(\eta_1, \eta_2, \eta_3).$$

Since at (η_1, η_2, η_3) all other pyramidal functions φ_v^0 , $v \in V^0$, take the value zero, we may write

$$\mathbf{1}_{S^2} = \sum_{v \in V^0} \varphi_v^0.$$

As a consequence, we can state that for every element g^{j-1} of the wavelet space \mathcal{W}^{j-1} ,

$$\langle \mathbf{1}_{S^2}, g^{j-1} \rangle_* = 0 \text{ for all } j \in \mathbb{N}^*.$$

This means that our wavelets have a vanishing moment of order zero with respect to the scalar product $\langle \cdot, \cdot \rangle_*$:

$$0 = \sum_{T \in \mathcal{T}^0} \int_{p(T)} g^{j-1}(\boldsymbol{\eta}) w_T(\eta_1, \eta_2, \eta_3) d\omega(\boldsymbol{\eta}),$$

with w_T the weight-functions given by (1).

Since

$$\begin{aligned} \langle \mathbf{1}_{S^2}, g^{j-1} \rangle_* &= \langle \mathbf{1}_{S^2} \circ p, g^{j-1} \circ p \rangle_\Omega = \langle \mathbf{1}_\Omega, g^{j-1} \circ p \rangle_\Omega \\ &= \sum_{T \in \mathcal{T}^0} \frac{1}{a(T)} \int_T (g^{j-1} \circ p)(\mathbf{x}) d\Omega(\mathbf{x}) \\ &= \frac{1}{3} \sum_{[w_1 w_2 w_3] \in \mathcal{T}^j} (g^{j-1} \circ p)(w_1) + (g^{j-1} \circ p)(w_2) + (g^{j-1} \circ p)(w_3) \\ &= \frac{1}{3} \sum_{w \in V^j} t(w) g^{j-1}(p(w)), \end{aligned}$$

we finally obtain

$$\sum_{w \in V^j} t(w) g^{j-1}(p(w)) = 0.$$

□

Next we apply this result to obtain another identity which show the fact that a sum of prewavelets ψ_u^{j-1} is constant over coarse and fine vertices.

Proposition 2. *Let*

$$\Sigma^{j-1}(\eta) = \sum_{u \in V^j \setminus V^{j-1}} t(u) \psi_u^{j-1}(\eta), \quad \eta \in \mathbb{S}^2.$$

Then we have

$$\Sigma^{j-1}(p(w)) = \begin{cases} 3 & \text{if } w \in V^j \setminus V^{j-1}, \\ -9 & \text{if } w \in V^{j-1}. \end{cases}$$

Proof. For $u \in V^j \setminus V^{j-1}$, the number of its neighbors is $t(u) = 6$. Therefore we can write the weighted sum as

$$\Sigma^{j-1}(\eta) = 6 \sum_{u \in V^j \setminus V^{j-1}} \psi_u^{j-1}(\eta).$$

First let w be a fine vertex, i.e. $w \in V^j \setminus V^{j-1}$. From the previous proposition we have

$$0 = \sum_{u \in V^j} t(u) \psi_w^{j-1}(p(u)) = \sum_{u \in V^j \setminus V^{j-1}} t(u) \psi_w^{j-1}(p(u)) + \sum_{v \in V^{j-1}} t(v) \psi_w^{j-1}(p(v)). \quad (10)$$

With w being the mid-point of an edge $[a_1 a_2]$, $a_1, a_2 \in V^{j-1}$, we obtain from (3) that

$$\begin{aligned} \sum_{v \in V^{j-1}} t(v) \psi_w^{j-1}(p(v)) &= \sum_{v \in V^{j-1}} t(v) \sigma_{a_1, w}^{j-1}(p(v)) + t(v) \sigma_{a_2, w}^{j-1}(p(v)) \\ &= t(a_1) \sigma_{a_1, w}^{j-1}(p(a_1)) + t(a_2) \sigma_{a_2, w}^{j-1}(p(a_2)) \\ &= -\frac{3}{2} - \frac{3}{2} = -3. \end{aligned} \quad (11)$$

The symmetry property $\psi_w^{j-1}(p(u)) = \psi_u^{j-1}(p(w))$ yields

$$\Sigma^{j-1}(p(w)) = \sum_{u \in V^j \setminus V^{j-1}} t(u) \psi_u^{j-1}(p(w)) = \sum_{u \in V^j \setminus V^{j-1}} t(u) \psi_w^{j-1}(p(u)) = 3,$$

taking into account (10) and (11).

Finally, let $v \in V^{j-1}$ be a coarse vertex. Then

$$\begin{aligned} \Sigma^{j-1}(p(v)) &= \sum_{u \in V^j} t(u) \sigma_{v, u}^{j-1}(p(v)) = -\frac{3}{2t(v)} \sum_{u \in V^j} t(u) \\ &= -\frac{3}{2t(v)} 6t(v) = -9. \end{aligned}$$

□

5. Some numerical tests

To illustrate the efficiency of our prewavelets, we took as the initial polyhedron the regular octahedron and we performed five levels of decomposition. The total number of vertices at the level five is 4098. We considered a data set *jump* consisting of 36×72 measurements on the sphere at the points $P_{ij}(\theta_i, \varphi_j)$, given by

TABLE 1. Reconstruction errors for some compression rates

comp. rate	nr. of zero coeff.	$\ \mathbf{e}^5\ _\infty$	$\ \mathbf{e}^5\ _2$	mean (\mathbf{e}^5)
0.05	3888	59.2191	992.7856	12.5437
0.1	3683	17.6250	220.3438	2.5425
0.25	3070	1.4023	12.9496	0.1287
0.5	2046	0.0527	0.4462	0.0039
0.75	1024	0.0005	0.0034	$1.97 \cdot 10^{-5}$

their spherical coordinates (θ, φ) , where $(\theta_i)_{1 \leq i \leq 36}$ are equidistant nodes of the interval $[-\pi, \pi]$ and $(\varphi_j)_{1 \leq j \leq 36}$ are equidistant nodes of the interval $[-\pi/2, \pi/2]$. This dataset is constant over the sphere, except to a small portion, where it has a very big jump (see Figure 1). Such functions appear in crystallography (see [6]).

First we approximated this data with the function $f^5 \in \mathcal{V}^5$ (figure 2). The measured approximation errors were

$$e_1 = \frac{1}{36 \cdot 72} \sum_{i=1}^{36} \sum_{j=1}^{72} |f^5(i, j) - \text{jump}(i, j)| = 1.0984,$$

$$e_2 = \left(\frac{1}{36 \cdot 72} \sum_{i=1}^{36} \sum_{j=1}^{72} |f^5(i, j) - \text{jump}(i, j)|^2 \right)^{1/2} = 0.4424.$$

Then we performed the decomposition, thresholding and reconstruction using the algorithms described in Section 2 and Section 3. We denoted by \mathbf{e}^5 the vector $\mathbf{f}^5 - \widehat{\mathbf{f}}^5 = (f_v^5 - \widehat{f}_v^5)_{v \in V^5}$ and we measured the errors

$$\begin{aligned} \|\mathbf{e}^5\|_\infty &= \max_{\eta \in \mathbb{S}^2} |\mathbf{e}^5(\eta)| = \max_{v \in V^5} |\mathbf{e}^5(v)|, \\ \|\mathbf{e}^5\|_2 &= \left(\sum_{v \in V^5} |f_v^5 - \widehat{f}_v^5|^2 \right)^{1/2}, \\ \text{mean}(\mathbf{e}^5) &= \frac{1}{|V^5|} \sum_{v \in V^5} |\mathbf{e}^5(v)|. \end{aligned}$$

The errors are tabulated in Table 1.

To compare our approach, whose strength is the locality of the prewavelets support, we took the case of spherical harmonic polynomials. For more details about spherical harmonics, see [4]. The basis functions are the polynomial kernels. Their supports are localized, but not local. An example of a polynomial kernel is given in Figure 5. Here we can see that its support covers the whole sphere. The wavelet decomposition was described in [1], Chapter 3. We performed 6 levels of decomposition. At the level $j = 6$, the total number of vertices was $2^{2j+1} = 8192$. Figure 6 show the approximation at the level 6. The oscillations around the jump, which occur because of the global support, are avoided in our approach.

Finally, let us mention that, to our knowledge, no construction of locally supported continuous prewavelets was made so far.

References

- [1] M. Conrad, *Approximation und Multiskalenzerlegung auf der Sphäre*, Diplomarbeit, Univ. Hamburg, 2001.
- [2] M. Floater, E. Quak, M. Reimers, *Filter bank algorithms for piecewise linear prewavelets on arbitrary triangulations*, Journal of Computational and Applied Mathematics, **119**(2000), 185-207.
- [3] M. Floater, E. Quak, *Linear Independence and Stability of piecewise linear prewavelets on arbitrary triangulations*, SIAM J. Numer. Anal. Vol., **38**, No. 1, 58-79.
- [4] W. Freeden, T. Gervens, M. Schreiner, *Constructive Approximation on the Sphere with Applications to Geomathematics*, Charendon Press, Oxford, 1988.
- [5] D. Roşca, *Locally supported rational spline prewavelets on a sphere*, submitted.
- [6] H. Schaeben, D. Potts, J. Prestin, *Spherical Wavelets with Application in Preferred Crystallographic Orientation*, IAMG' 2001, Cancun, 2001.
- [7] G. Strang, T. Nguyen, *Wavelets and Filter Banks*, Wellesley-Cambridge Press, Wellesley, 1996.

DANIELA ROȘCA

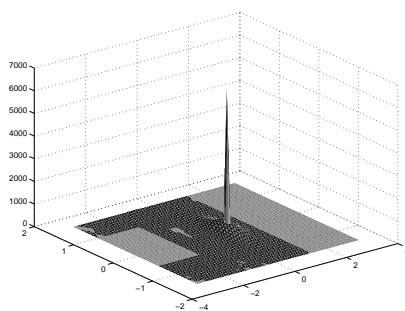


FIGURE 1. The initial dataset $jump$, represented in spherical coordinates.

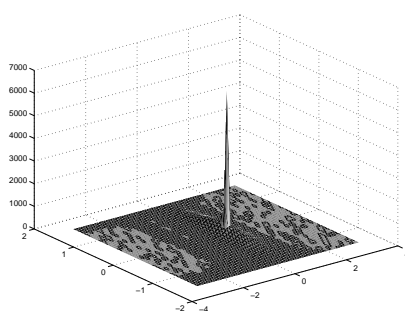


FIGURE 2. The approximation f^5 at the level 5.

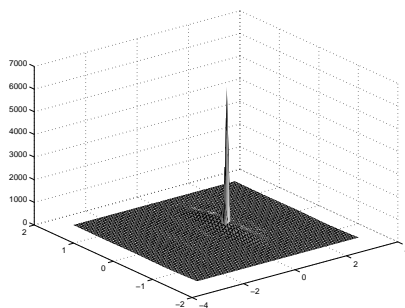


FIGURE 3. Approximation with the compression rate 0.05.

TECHNICAL UNIVERSITY OF CLUJ-NAPOCA, STR. DAICOVICIU NR. 15,
3400 CLUJ-NAPOCA, ROMANIA
E-mail address: Daniela.Catinas@math.utcluj.ro

ALGORITHMS FOR APPROXIMATION

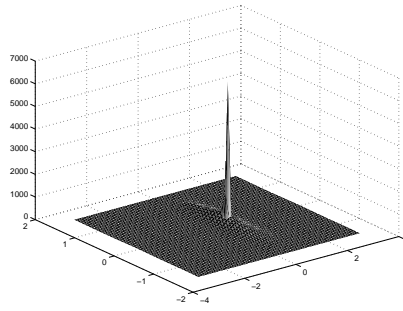


FIGURE 4. Approximation with the compression rate 0.1.

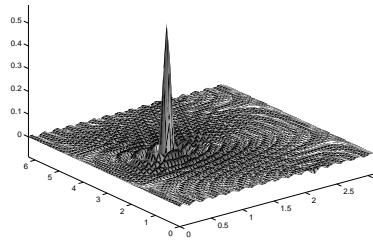


FIGURE 5. An example of kernel of spherical harmonics: localized but supported on the whole sphere.

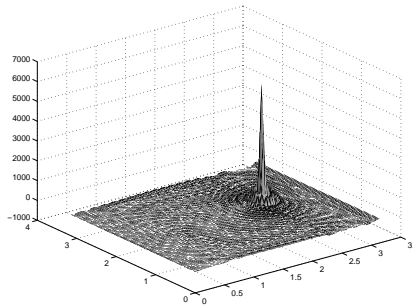


FIGURE 6. Approximation at the level 6, using the kernels of spherical harmonics.